ISSN 1063-7826, Semiconductors, 2016, Vol. 50, No. 1, pp. 59–65. © Pleiades Publishing, Ltd., 2016.
Original Russian Text © S.Z. Zaynabidinov, A.S. Saidov, A.Yu. Leiderman, M.U. Kalanov, Sh.N. Usmonov, V.M. Rustamova, A.Y. Boboev, 2016, published in Fizika i Tekhnika Poluprovodnikov, 2016, Vol. 50, No. 1, pp. 60–66.

SURFACES, INTERFACES, AND THIN FILMS

Growth, Structure, and Properties of GaAs-Based $(GaAs)_{1-x-y}(Ge_2)_x(ZnSe)_y$ Epitaxial Films

S. Z. Zaynabidinov[a]*, A. S. Saidov[b], A. Yu. Leiderman[b], M. U. Kalanov[c], Sh. N. Usmonov[b], V. M. Rustamova[c], and A. Y. Boboev[a, c]

[a] *Babur Andizhan State University, Andizhan, 170100 Uzbekistan*
[b] *Starodubtsev Physical–Technical Institute, Tashkent, 100084 Uzbekistan*
[c] *Institute of Nuclear Physics, Academy of Sciences of the Republic of Uzbekistan, Tashkent, 100214 Uzbekistan*
* *e-mail: prof_sirojiddin@mail.ru*

Submitted March 31, 2015; accepted for publication April 20, 2015

Abstract—The possibility of growing the $(GaAs)_{1-x-y}(Ge_2)_x(ZnSe)_y$ alloy on GaAs substrates by the method of liquid-phase epitaxy from a tin solution–melt is shown. X-ray diffraction shows that the grown film is single-crystal with the (100) orientation and has the sphalerite structure. The crystal-lattice parameter of the film is $a_f = 0.56697$ nm. The features of the spectral dependence of the photosensitivity are caused by the formation of various complexes of charged components. It is established that the I–V characteristic of such structures is described by the exponential dependence $I = I_0\exp(qV/ckT)$ at low voltages (no higher than 0.4 V) and by the power dependence $J \sim V^{\alpha}$, where the exponent α varies with increasing voltage at high voltages ($V > 0.5$ V). The results are treated within the framework of the theory of the drift mechanism of current transfer taking into account the possibility of the exchange of free carriers within the recombination complex.

DOI: 10.1134/S1063782616010231

1. INTRODUCTION

It is known that the semiconductor heterostructures are now widely used for fabricating detectors and converters of optical radiation—they are an integral component of such important optoelectronic devices as heterojunction lasers. This has resulted in the intense development of the physics and technology of two-layer and multilayer semiconductor heterostructures. Nowadays, three methods are predominantly used to obtain semiconductor heterostructures: liquid-phase epitaxy (LPE), chemical vapor deposition (CVD), and molecular-beam epitaxy (MBE). In the most widely used method LPE, an epitaxial layer is deposited from a solution–melt, which is in contact with the surface of a substrate for obtaining A^{III}–B^{V} films. As a solvent, elements of Group III of the periodic table are used more often. CVD is used mainly for growing epitaxial heterostructures on the basis of A^{III}–B^{V} semiconductors. In MBE, epitaxial layers are grown by deposition onto a substrate of atoms or molecules, the fluxes of which are formed in ultrahigh vacuum. In all methods, a necessary condition for obtaining high-quality heterostructures is compatibility of the lattice parameters of the substrate and the film, and also of the coefficients of linear thermal expansion of the materials [1, 2]. The physical properties of heterostructures and the characteristics of devices on their basis depend mainly on the internal stresses and defects in the epitaxial layers. Thus, determination of the optimum technological conditions, the structural parameters, and the physical properties of particular heterostructures is important from both physical and technological viewpoints. In this context, we present here the results of investigations carried out over the last years on the growth conditions, the structure, and the physical characteristics of the $(GaAs)_{1-x-y}(Ge_2)_x(ZnSe)_y$ semiconductor alloy.

2. GROWTH TECHNIQUE FOR EPITAXIAL LAYERS OF $(GaAs)_{1-x-y}(Ge_2)_x(ZnSe)_y$ ON A GaAs SINGLE-CRYSTAL SUBSTRATE

The epitaxial layers under investigation were grown by the method of liquid-phase epitaxy with the technique described in [3]. As substrates, we used GaAs washers 20 mm in diameter and ~350 μm thick, which were cut from single-crystal n-GaAs with the (100) orientation and doped with tin with a concentration of $(3–5) \times 10^{17}$ cm^{-3} with the resistivity $\rho = 250$ Ω cm. The solution–melt composition was obtained on the basis of preliminary investigations of the GaAs–ZnSe–Sn–Ge system and published data from [4, 5]. The layers were grown from the tin solution–melt by forced cooling in an atmosphere of hydrogen purified with palladium. The forced-cooling rate under optimal conditions amounted to 1–

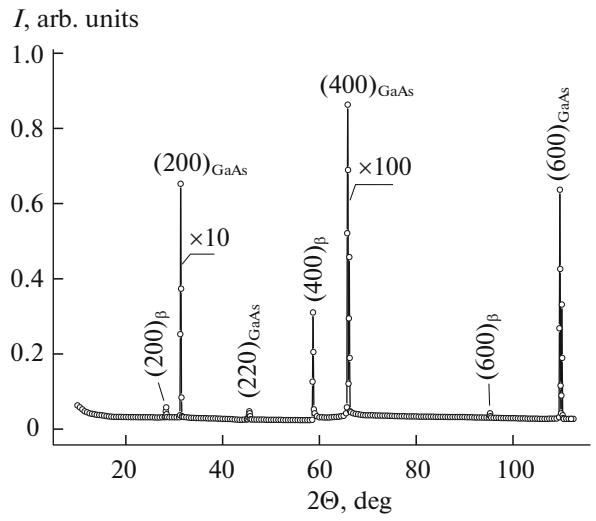

Fig. 1. X-ray diffraction pattern of the GaAs substrate.

1.5 deg/min. Layers of the $(GaAs)_{1-x-y}(Ge_2)_x(ZnSe)_y$ alloys were crystallized in the temperature range of 730–640°C and with a growth rate of ϑ = 0.15 μm/min. At the initial moment of growth from the solution–melt, GaAs is crystallized because the solution is saturated in relation to GaAs at the chosen epitaxy temperature. At lower temperatures, conditions are implemented for the growth of $(GaAs)_{1-x-y}(Ge_2)_x(ZnSe)_y$ alloy because the solution–melt becomes supersaturated with the elements Ge and ZnSe at these temperatures. The grown epitaxial layers had *p*-type conductivity, and the layer thickness amounted to $d \approx 10$ μm.

It is known that the value of the covalent radii of the elements plays a substantial role during the growth of epitaxial films of complex composition. In this case, the sums of the covalent radii of atoms in the GaAs, Ge_2, and ZnSe molecules have close values:

$$\begin{aligned}\Delta r_1 &= |(r_{Ga} + r_{As}) - (r_{Ge} + r_{Ge})| = |2.41\text{Å} - 2.41\text{Å}| = 0,\\ \Delta r_2 &= |(r_{Ga} + r_{As}) - (r_{Zn} + r_{Se})|\\ &= |2.41\text{Å} - 2.42\text{Å}| = 0.01\text{Å} < 0.1(r_{Ga} + r_{As}),\\ \Delta r_3 &= |(r_{Ge} + r_{Ge}) - (r_{Zn} + r_{Se})|\\ &= |2.41\text{Å} - 2.42\text{Å}| = 0.01\text{Å} < 0.1(r_{Ga} + r_{As}),\end{aligned} \quad (1)$$

where $r_{Ga} = 1.22$ Å, $r_{As} = 1.19$ Å, $r_{Ge} = 1.205$ Å, $r_{Zn} = 1.22$ Å, and $r_{Se} = 1.20$ Å are the covalent radii of gallium, arsenic, germanium, zinc, and selenium atoms from the data in [6]. It can be seen from (1) that the difference in the values of the sums of the covalent radii of atoms of GaAs, Ge_2, and ZnSe molecules are insignificant, result in no substantial deformation of the crystal lattice, and satisfy the conditions of the formation of a continuous substitutional solid solution [7]. In addition, the sum of the atomic valences in the component molecules is mutually equal, which is also of importance for satisfying the conditions for electroneutrality:

$$\begin{aligned}\Delta z_1 &= |(z_{Ga} + z_{As}) - (z_{Ge} + z_{Ge})| = 0,\\ \Delta z_2 &= |(z_{Ga} + z_{As}) - (z_{Zn} + z_{Se})| = 0,\\ \Delta z_3 &= |(z_{Ge} + z_{Ge}) - (z_{Zn} + z_{Se})| = 0,\end{aligned} \quad (2)$$

where $z_{Ga} = +3$, $z_{As} = +5$, $z_{Ge} = +4$, $z_{Zn} = +2$, and $z_{Se} = +6$ are the valences of gallium, arsenic, germanium, zinc, and selenium atoms, respectively. Thus, two important conditions for the formation of a continuous substitutional solid solution [7] are satisfied in our experiments.

3. STRUCTURAL CHARACTERISTICS AND PHOTOELECTRIC PROPERTIES OF *n*-GaAs–*p*-$(GaAs)_{1-x-y}(Ge_2)_x(ZnSe)_y$ HETEROSTRUCTURES

The obtained structures were investigated both on the substrate and film sides at 300 K using a DRON-3M X-ray diffractometer (CuK_α-radiation, $\lambda = 0.15418$ nm) according to the θ–2θ scheme in the mode of step-by-step scanning. In Fig. 1, we show the X-ray diffraction pattern of the GaAs substrate. It can be seen that there are several selective structural reflections with different intensities in the diffraction pattern. The analysis showed that the substrate surface corresponds to the (100) crystallographic plane. The presence of a series of selective reflections of the {*H*00} type (where $H = 1$, 2, 3...) with high intensities on the X-ray diffraction pattern is evidence of this; the structural lines are $(200)_{GaAs}$ with $d/n = 0.2814$, $(400)_{GaAs}$ with $d/n = 0.1412$, and $(600)_{GaAs}$ with $d/n = 0.09422$ nm. Their β components can be seen at the scattering angles 2θ = 28.2°, 2θ = 58.8°, and 2θ = 95.2°, respectively. In the diffraction spectrum at average scattering angles, the structural reflection $(220)_{GaAs}$ with $d/n = 0.1998$ nm is still observed at 2θ = 45.4° with a low intensity. The high intensity (2×10^5 pulse s^{-1}) of the main reflection $(400)_{GaAs}$, a relatively narrow width (FWHM = 0.0039 rad), and the flat minimum of the inelastic background are evidence of a high degree of perfection of the substrate crystal lattice. The experimentally determined value of the substrate lattice parameter is $a_{GaAs} = 0.56532$ nm, which is very close to its tabulated value of $a_{GaAs} = 0.5646$ nm [8].

In Fig. 2, we show the X-ray diffraction pattern of an epitaxial film of the $(Ge_2)_{1-x-y}(GaAs)_x(ZnSe)_y$ solid solution. It substantially differs from the X-ray diffraction pattern for the substrate and an increase in the intensity of the main reflection (400) at 4.5% is observed in it; the intensities of reflections (200) and (600) are increased by 1.7 and 1.4 times, respectively, and the intensity of the reflection (220) is increased insignificantly. New structural lines with d/n = 0.1268 nm (2θ = 74.9°), $d/n = 0.1263$ nm (2θ = 75.2°) and $d/n = 0.1001$ nm (2θ = 100.8°) are simultaneously

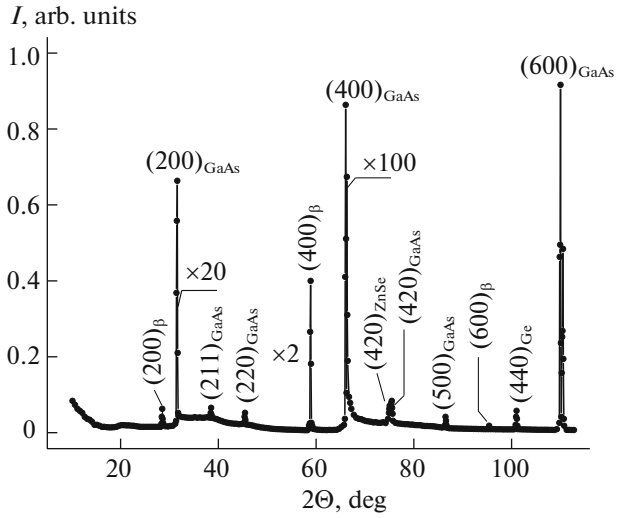

Fig. 2. X-ray diffraction pattern of the $(GaAs)_{1-x-y}(Ge_2)_x(ZnSe)_y$ epitaxial film.

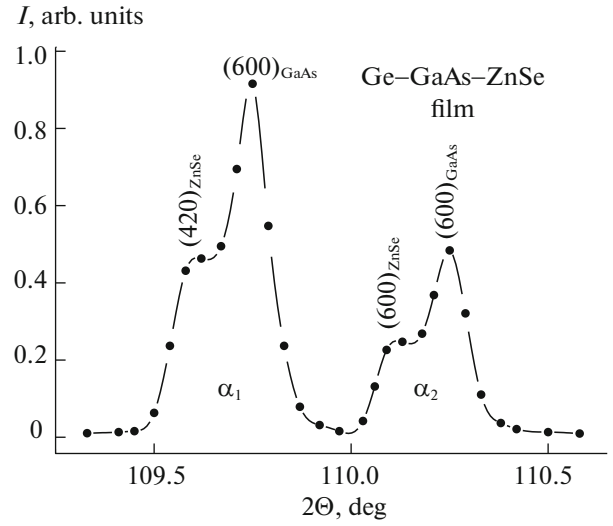

Fig. 3. Shape of reflection (600) from the $(GaAs)_{1-x-y}(Ge_2)_x(ZnSe)_y$ film.

observed, as well as nonmonotonic character of the inelastic-background level in the regions of small and average scattering angles. A relatively narrow width (FWHM = 4.36×10^{-3} rad) and a high intensity (2×10^5 pulse s^{-1}) of the main reflection (400), and also the presence of other even orders of reflection on the X-ray diffraction pattern, testify to a high degree of perfection of the film crystal lattice; this means that the grown film has the sphalerite structure (ZnS-type structure) and is single-crystal with the (100) orientation. The size of subcrystallites (blocks) in the film estimated from the width of this peak amounts to about 52 nm.

Appreciable splitting of this reflection into α_1 and α_2 radiation components, but less than their calculated values $\{I((\alpha_1) = 2I(\alpha_2)\}$ points to the presence of insignificant elastic microstresses in the film lattice. Lattice microdistortions and a somewhat larger value of the intensity of reflections $(H00\}$ (where $H = 2, 4, 6$) than the intensities of the same lines of the substrate testify to the partial replacement of some GaAs molecules with Zn, Se, and Ge molecules in its imperfect regions, i.e., at the boundaries and near-boundary interfaces of blocks. This is confirmed by the fact that the film lattice parameters determined from three reflections, i.e., (200), (400), and (600) with the help of the Nelson–Relay extrapolation function $\xi = (1/2) \times [(\cos^2\theta/\theta + (\cos^2\theta/\sin\theta)] - a_f = 5.6568$ Å are somewhat larger than the substrate lattice parameter $a_s = 5.6532$ Å. Additional confirmation of this is the presence of weak forbidden reflections (211) with $d/n = 0.2305$ nm ($2\theta = 38.5°$) and (500) with $d/n = 0.1128$ nm ($2\theta = 86.1°$) on the X-ray diffraction pattern for sphalerite structures, the intensities of which are related to the intensities of the main peak (400) as $I(211)/I(400) = 4.73 \times 10^{-4}$ and $I(500)/I(400) = 2.74 \times 10^{-4}$, respectively [9]. However, the level of inelastic background near the structural reflections (200) and (400) is 22% higher than the background level in similar angular ranges for the substrate. This testifies to the local character of the elastic-energy concentration in the film lattice and the presence of microdistortions in much smaller quantities (it is possible that they are the consequence of the proximity of the ionic radii of film elements: $r_{Zn} = 0.074$ nm, $r_{Se} = 0.050$ nm, $r_{As} = 0.058$ nm, $r_{Ga} = 0.062$ nm, and $r_{Ge} = 0.053$ nm) [10].

Apparently, such small distortions of the lattice stimulate the formation of nanoinclusions of various phases for energy stabilization of the film. Investigations of the shapes of diffraction reflections (600) showed that they are resolved into α_1 and α_2 radiation components for the GaAs and ZnSe lattice, respectively (Fig. 3). The existence of such distortions of the crystal lattice of the films under investigation is probably the cause of the formation of various nanoformations. Confirmation of the formation of nanoinclusions in the crystal lattice lies in the occurrence of several new selective reflections with a significant intensity in the diffraction pattern. Analysis showed that new structural lines with $d/n = 0.1268$ nm ($2\theta = 74.9°$) and $d/n = 0.1263$ nm ($2\theta = 75.2°$) are diffraction reflections from the planes (420) of the crystal lattices of ZnSe and GaAs nanocrystals with sizes of ~59 and ~48 nm, respectively. The structural peak (440) with $d/n = 0.1001$ nm ($2\theta = 100.8°$) belongs to the crystal lattice of Ge nanocrystals ~44 nm in size. The experimentally determined values of the parameters of zinc-selenide and gallium-arsenide lattices amounted to $a_{ZnSe} = 5.6697$ Å and $a_{GaAs} = 5.6697$ Å, which are close to their tabulated values of $a_{ZnSe} = 5.661$ Å and

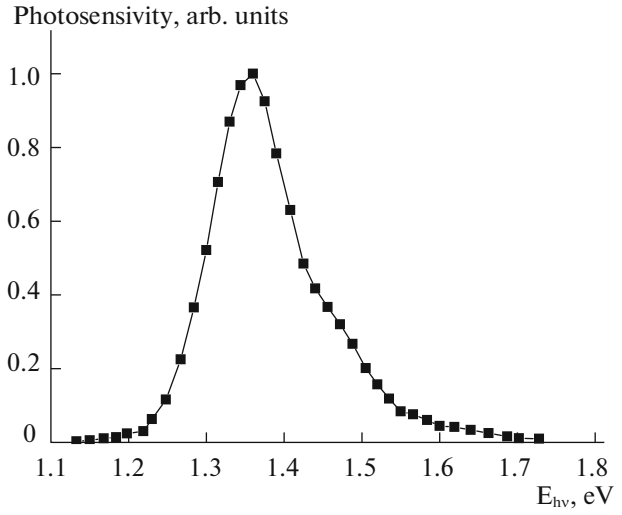

Fig. 4. Spectral photosensitivity of the *n*-GaAs–*p*-$(GaAs)_{1-x-y}(Ge_2)_x(ZnSe)_y$ structure at 300 K.

a_{GaAs} = 5.646 Å, respectively [9]. The lattice constant of Ge nanocrystals determined from the X-ray diffraction pattern amounted to a_{Ge} = 5.6625 Å, which is also close to its tabulated value of a_{Ge} = 5.6576 Å [9]. Thus, the investigations showed that the epitaxial layers of $(GaAs)_{1-x-y}(Ge_2)_x(ZnSe)_y$ alloy obtained using the above technology on GaAs with a thickness of 10 μm have structural perfection of a reasonably high degree, the sphalerite structure, and are single-crystal with block sizes of 52 nm and an orientation corresponding to that of the substrate; ZnSe and Ge molecules in part replace GaAs molecules in imperfect regions of the matrix lattice at the boundaries and near-boundary regions of phases and at the interfaces between with subsequent segregation of Ge ions and ZnSe molecules and the formation of nanocrystals at these places.

To determine the role of components of alloys in the processes under observation, we studied the spectral dependences of the photosensitivity of the fabricated structures with the help of a mirror–prism monochromator with quartz optics, which enabled us to investigate the samples in the radiation-wavelength range from 0.35 to 2.5 μm. In Fig. 4, we show the spectral dependence of the photosensitivity of the *p*-(GaAs)–*n*-$(GaAs)_{1-x-y}(Ge_2)_x(ZnSe)_y$ structures from which it can be seen that the photosensitivity of the investigated structures covers the photon-energy range from 1.13 to 1.73 eV. The photosensitivity of the investigated structure originates at photon energies of 1.13 eV. It is probably caused by the narrow-gap component Ge_2 in the $(GaAs)_{1-x-y}(Ge_2)_x(ZnSe)_y$ alloy [11]. Since Ge_2 and ZnSe components replace Ga and As atoms in the GaAs tetrahedral lattice [7], the Ga–As bonds are weakened under the effect of Ge atoms surrounding them. Since the binding energy of the Ge–Ge molecule, when it is in the tetrahedral lattice, depends on the Ge band-gap width (E_{Ge} = 0.67 eV), and it is smaller than the GaAs band-gap width (E_{GaAs} = 1.42 eV), the ionization energy of the Ge–Ge bond increases, when it is surrounded with GaAs, and the wide-gap ZnSe component only slightly affects the GaAs band-gap width. The maximum spectral photosensitivity of the $(GaAs)_{1-x-y}(Ge_2)_x(ZnSe)_y$ alloy is observed at 1.34 eV, which is less than the GaAs band gap. However, the increase in the spectral sensitivity is not abrupt, which is probably due to the layer thickness of the $(GaAs)_{1-x-y}(Ge_2)_x(ZnSe)_y$ alloy efficiently absorbing low-energy photons. The decrease in the photosensitivity at photon energies higher than 1.34 eV, in our opinion, is caused by the location depth of the separation barrier of the *p–n* junction, which depends on the epitaxial-layer thickness amounting to ~10 μm. The diffusion length of minority charge carriers in the $(GaAs)_{1-x-y}(Ge_2)_x(ZnSe)_y$ layer amounts to ~4.8 μm, which is much smaller than the location depth of the separation barrier, corresponding to our assumption.

4. FEATURES OF THE CURRENT–VOLTAGE (*I–V*) CHARACTERISTICS OF *n*-GaAs–*p*-$(GaAs)_{1-x-y}(Ge_2)_x(ZnSe)_y$ STRUCTURES

To study the *I–V* characteristics of the structures, we used the method of vacuum deposition for the fabrication of ohmic contacts to the structures—continuous contacts on the rear side and silver contacts in the form of a quadrilateral 9 mm^2 in area on the epitaxial-layer side. The "dark" *I–V* characteristics were measured at temperatures of 300–380 K.

The initial portion of the *I–V* characteristics from zero to 0.25 V is ohmic, i.e., the dependence $J \propto V$ takes place. With increasing applied voltage in the range from 0.25 to 0.4 V, an exponential dependence (Fig. 5) is observed. The *I–V* characteristic is described irrespective of the temperature by the expression:

$$I \approx I_0 e^{\frac{qV}{ckT}}. \quad (3)$$

The factor "*c*" in the exponent of the *I–V* characteristic is determined from the experimental data as

$$c = \frac{q}{kT}\frac{V_2 - V_1}{\ln\frac{I_2}{I_1}}. \quad (4)$$

The exponential dependence of the current on the voltage for the first time was predicted by Stafeev [12]

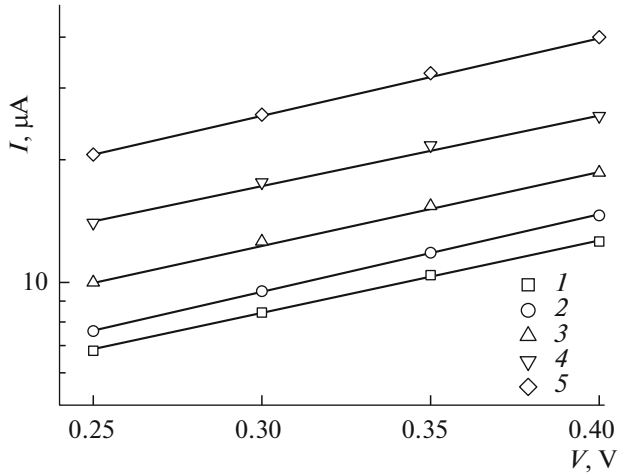

Fig. 5. "Dark" I–V characteristic of the n-GaAs–p-$(GaAs)_{1-x-y}(Ge_2)_x(ZnSe)_y$ structures on the semilogarithmic scale at the temperatures T = (*1*) 300, (*2*) 320, (*3*) 340, (*4*) 360, and (*5*) 380 K.

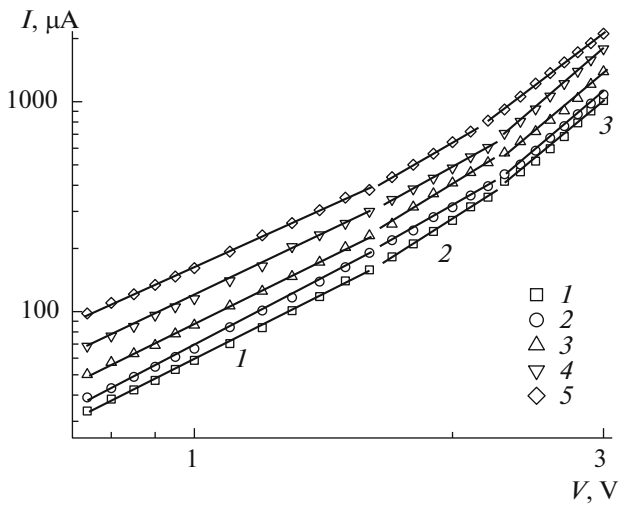

Fig. 6. Typical I–V characteristic of the n-GaAs–p-$(GaAs)_{1-x-y}(Ge_2)_x(ZnSe)_y$ structures on the logarithmic scale at different temperatures T = (*1*) 300, (*2*) 320, (*3*) 340, (*4*) 360, and (*5*) 380 K.

and, then, was refined in [13] for p–i–n structures with c in the exponent, which has the following form:

$$c = \frac{2b + \cosh(W/L_n) + 1}{b + 1}, \qquad (5)$$

where $b = \mu_n/\mu_p$ is the ratio of the mobilities of electrons and holes for the $(GaAs)_{1-x-y}(Ge_2)_x(ZnSe)_y$ alloy and is equal to $b \approx 3.1$. Knowing b, we can find $W/L_n = 4.16$; then, it is possible to calculate the diffusion length of minority charge carriers $L_n = 4.8$ μm. This enables us to determine the product $\mu_n\tau_n = qL_n/kT$, which at room temperature is equal to ~8.9×10^{-10} cm^2/V. The mobility of majority charge carriers μ_p determined by the Hall method amounted to ~360 cm^2/(V s). On the basis of these data, we determined the values of I_0, c, and b at various temperatures, which are listed in Table 1. As can be seen from Table 1, at temperatures of 300–360°C, the values of I_0 (A) gradually increase and barely depend on c and b. At 380 K, an appreciable increase in their value is observed. This is probably associated with the varying concentration of centers affecting the mobility of charge carriers at 300–360 K. At a temperature of 380 K, the formation of various charged centers which scatter charge carriers and change their mobility is possible. The results of the calculations are listed in Table 1. As can be seen from Fig. 6, the I–V characteristics of these structures at a voltage of $V > 0.5$ V are described by the power dependence $J \propto V^\alpha$, where α varies from two to three and increases with voltage. The first portion $J \propto V^2$ is observed in the voltage range from 0.5 to 1.7 V and can be accounted for within the framework of the concept of the drift mode of ohmic relaxation of the space charge [14]. With a further increase in voltage, we observed a sharp increase in the current in the form of $J \propto V^{2.7}$. Apparently, the processes of intracomplex electron exchange resulting in a "delay" in the onset of recombination processes to play the role here. In other words, the recombination rate of free carriers is no longer subjected to Shockley–Read statistics, and further takes a complex form [15, 16]:

$$u_r = N_r \frac{c_n c_p (pn - n_i^2)}{c_n(n + n_1) + c_p(p + p_1) + \alpha\tau_i pn}, \qquad (6)$$

where N_r is the concentration of recombination centers; n and p are the electron and hole concentrations; n_i is the intrinsic concentration of charge carriers in the semiconductor; c_n and c_p are the capture cross sections for electrons and holes, respectively; n_1 and p_1 are the equilibrium electron and hole concentration in the case where the Fermi level coincides with the impurity

Table 1. Values of the pre-exponential multiplier I_0, the parameter c in the exponent of expression (3), and the ratio of the mobilities of electrons and holes for n-GaAs–p-$(GaAs)_{1-x-y}(Ge_2)_x(ZnSe)_y$ heterostructures at various temperatures

T, K	300	320	340	360	380
I_0, (A)	2.6×10^{-6}	3.63×10^{-6}	4.43×10^{-6}	6.73×10^{-6}	5.54×10^{-6}
c	9.56	9.65	9.55	9.62	10.55
d	3.1	3.05	3.14	3.102	5.38

Table 2. Values of parameters A, B, and D in expression (8) at various temperatures

T, K	300	320	340	360	380
B	3.1	3.05	3.14	3.1	5.38
A, (B)	2.65	2.67	2.69	2.74	2.63
D, (V m $A^{-1/2}$)	13.25	15.9	21.67	23.97	22.7
B, (V $A^{1/2}$ m^{-1})	13.07	15.7	21.5	23.8	22.5

level; $\alpha\tau_i pn$ is the term describing intracomplex exchange; and τ_i is the intracomplex-exchange time. This term in the denominator of expression (6) increases with excitation level. At a low excitation level, this term is negligibly small, and the recombination rate is described by Shockley–Read statistics. In this case, the I–V characteristic in the drift mode of the current transfer has the usual quadratic form; i.e., $\alpha_1 = 2$ corresponding to ohmic relaxation of the space charge [14]:

$$V = \sqrt{\frac{8d^2J}{9q\mu_n\mu_p\tau_pN_D}} = B_0\sqrt{J}, \qquad (7)$$

where $\mu_p = 360$ cm^2/(V s) and $\tau_p = 2.5 \times 10^7$ are the mobility and the lifetime of holes; $\mu_n = 1113$ cm^2/(V s) is the mobility of electrons; J is the current density; $d = 10$ μm is the base thickness; and $N_D = 1.4 \times 10^{15}$ cm^{-3} is the concentration of shallow donor impurity centers. From the slope of the dependence $J \propto V^2$, we determined the value of B_0, which amounted to $B_0 = 59.23$ V cm A^{-1}.

The next portion of the I–V characteristics, $J \propto V^\alpha$, where $\alpha = 2.7$ is observed at voltages from 1.7 to 2.2 V, when the recombination of nonequilibrium charge carriers occurs mainly with a delay; i.e., the last term in the denominator of Eq. (6) becomes substantial. In this case, the I–V characteristic has the following analytical expression [14]:

$$V = \frac{(b+1)d^2N_R}{N_D\mu_p\tau_i} + \frac{d}{q\mu_p(b+1)C}\sqrt{J} - \frac{2(b+1)N_Rd^2c_n}{N_D\mu_p\alpha\tau_iC}\frac{1}{\sqrt{J}} = A + B\sqrt{J} - \frac{D}{\sqrt{J}}, \qquad (8)$$

where A, B, and D are parameters dependent on the concentration of ionized atoms of deep impurities, the ratio of the electron and hole mobilities, and the thickness of the interlayer-junction base, respectively. In Table 2, we list the values of the parameters A, B, and D depending on temperature. As can be seen from Table 2, the parameters A, B, and D determining the value of V and dependent on the concentration of ionized atoms, i.e., on the concentration of recombination centers N_R, the mobilities of charge carriers, and the thickness of the interlayer-junction base gradually increase in the range 300–360 K and appreciably decrease at 380 K. Such behavior is probably related to the significant effect of the intracomplex-exchange time τ on these processes.

Beyond this portion (see Fig. 6), the I–V characteristic has the form $J = A_1V^3$ at voltages from 2.2 to 3 V. This is the portion of the I–V characteristic subjected to the Lampert law

$$J = \frac{125\varepsilon\tau\mu_n\mu_p}{18}\frac{V^3}{d^3} \qquad (9)$$

and referred to as the drift mode of dielectric relaxation.

5. CONCLUSIONS

Thus, on the basis of analysis of the technological modes of the synthesis of epitaxial layers of the $(GaAs)_{1-x-y}(Ge_2)_x(ZnSe)_y$ alloy on GaAs substrates and the results of the performed investigations, it is possible to make the following conclusions.

(i) The optimum technological modes are determined for the growth of structurally perfect epitaxial layers of the $(GaAs)_{1-x-y}(Ge_2)_x(ZnSe)_y$ alloy 10 μm thick on GaAs substrates (cooling rate of 1–1.5 deg/min, temperature of 730–640°C, and growth rate of $\vartheta = 0.15$ μm/min).

(ii) The grown $(GaAs)_{1-x-y}(Ge_2)_x(ZnSe)_y$ films have the sphalerite structure and are single-crystal with blocks 52 nm in size and an orientation corresponding to the (100) substrate orientation.

(iii) ZnSe and Ge molecules are apparently in part replaced with GaAs molecules in imperfect regions of the matrix lattice at the boundaries and near-boundary regions of phases and at the interfaces between with the subsequent segregation of germanium ions and zinc-selenide molecules and the formation of nanocrystals.

(iv) Electron–hole pairs generated in the near-surface region of the structure by short-wavelength photons do not reach the separation barrier and do not participate in the appearance of photocurrent, which is the principal cause of a drop in the photosensitivity of the structure under investigation in the short-wavelength region of the radiation spectrum.

(v) The current–voltage characteristic $J \propto V^\alpha$ of the n-GaAs–p-$(GaAs)_{1-x-y}(Ge_2)_x(ZnSe)_y$ heterostructures in the forward-current direction consists of several portions in which α has various values. This is probably related to the formation of composite recombination complexes of the type of negatively-charged acceptor–positively-charged interstitial ion or positively-charged donor–negatively-charged vacancy, which results in a "delay" in the recombination processes.

(vi) In such alloys, the recombination rate is determined also by the local centers of nanoformations or the simultaneous participation of complexes and local

centers instead of only by the nature of the complexes and simple charged centers.

ACKNOWLEDGMENTS

This study was supported by grant no. FA-F-F120 of the Committee on the coordination and development of science and technology of the Government of Republic of Uzbekistan.

REFERENCES

1. Zh. I. Alferov, Rev. Mod. Phys. **73**, 767 (2001).
2. S. L. Sheng, *Semiconductor Physical Electronics* (Springer, Berlin, 2006).
3. A. S. Saidov, A. Sh. Razzakov, V. A. Risaeva, and E. A. Koschanov, Mater. Chem. Phys. **68**, 1 (2001).
4. V. M. Andreev, L. M. Dolginov, and D. N. Tret'yakov, *Liquid Epitaxy in Technology of Semiconductor Devices* (Sov. Radio, Moscow, 1975) [in Russian].
5. A. S. Saidov, M. S. Saidov, and E. A. Koshchanov, *Liquid Epitaxy of Compensated Layers of Gallium Arsenide and Solid Solutions Based on it* (Fan, Tashkent, 1986) [in Russian].
6. *Chemist's Manual*, Ed. by B. P. Nikol'skii (Khimiya, Moscow, Leningrad, 1982) [in Russian].
7. M. S. Saidov, Geliotekhnika, No. 3, 4 (2001).
8. S. S. Gorelik, L. N. Rastorguev, and Yu. A. Skakov, *X-Ray and Electronic Optical Analysis* (Metallurgiya, Moscow, 1970) [in Russian].
9. I. L. Shul'pina, R. N. Kyutt, V. V. Ratnikov, I. A. Prokhorov, I. Zh. Bezbakh, and M. P. Shcheglov, Tech. Phys. **55**, 537 (2010).
10. *Short Handbook of Physical Chemical Quantities*, Ed. by A. A. Ravdel' and A. M. Ponomareva (Khimiya, Leningrad, 1983) [in Russian].
11. K. A. Amonov, in *Proceedings of the 48th International Scientific Student Conference* (Novosibirsk, 2010), p. 182.
12. V. I. Stafeev, Sov. Tech. Phys. **3**, 1502 (1958).
13. E. I. Adirovich, P. M. Karageorgij-Alkalaev, and A. Yu. Leiderman, *Double Injection Currents in Semiconductors* (Sov. Radio, Moscow, 1978) [in Russian].
14. R. Lampert and P. Mark, *Current Injection in Solids* (Academic Press, New York, 1970; Mir, Moscow, 1973).
15. A. Yu. Leiderman, in *Physics and Materials Science of Semiconductors with Deep Levels*, Ed. by V. I. Fistul (Metallurgiya, Moscow, 1987), p. 232 [in Russian].
16. A. Yu. Leiderman and M. K. Minbaeva, Semiconductors **30**, 905 (1996).

Translated by V. Bukhanov